

THERMAL ANALYSIS OF A MEMS BASED BROADBAND LIGHT SOURCE: TEST DATA AND MODEL

Eric L. Golliher¹, Margaret Tuma¹, Joseph Collura², Eric Jones³, James Yuko¹

¹NASA Glenn Research Center
21000 Brookpark Road
Cleveland, Ohio, 44135
Phone: (216) 433-6575
Email: golliher@grc.nasa.gov

²John Carroll University
20700 Northpark Blvd.
University Heights, OH 44118
Email: jcollura@jcu.edu

³Jet Propulsion Laboratory
4800 Oak Grove Dr.
Pasadena, CA 91109
E-mail: eric.jones@jpl.nasa.gov

ABSTRACT

NASA Glenn Research Center, the Jet Propulsion Laboratory and Lighting Innovations Institute at John Carroll University are developing a MEMS-based, low-power, incandescent broadband light source for aeronautics and spacecraft applications. This paper summarizes a thermal analysis of the MEMS package and filament. The packaged device is very small, measuring approximately 1.2 mm thick, 15 mm long, and 10 mm wide. This device can be used to interrogate optical sensors or as a calibration light source for spectrometers. Several alternating layers of Silicon, Silicon Nitride, Silver Oxide, and Titanium/Platinum/Gold build the basic mechanical structure. A square cavity in the center of this “box” suspends a spiral Tungsten filament. The filament emits light and heat like a black body at about 2650 K that bounces off the reflective walls of the cavity and exits through the Silicon Nitride window at the “top” of the structure. Temperature requirements, analysis methods and results are discussed. The analytical results are compared to recent laboratory test data.

KEY WORDS: blackbody, power, Silicon, Tungsten

NOMENCLATURE

A Area, m²
r Radius of spiral, microns
t Thickness of filament, m

Greek symbols

σ Stefan-Boltzman constant, W/m²•K⁴
 ϵ Emittance
 \dot{q} Heat Generation per unit volume, W/m³
 k Thermal Conductivity, W/mK
 x Length Along Filament, m
T Temperature, K

ρ Electrical resistivity (micro-ohms-cm)
 θ Spiral angle (radians)
 A_x Area perpendicular to the x direction, m
 w Filament width, m

INTRODUCTION

The development of a MEMS-based broadband lightsource has many technical challenges. The thermal design of the device was identified as critical to reliability and robustness [1]. This paper is concerned with the thermal analysis of the filament, fabricated by The Aerospace Corporation, and the associated portion of the package near the filament. Test data of a filament is compared to preliminary thermal analysis results. Further package level thermal analysis shows the impact of the hot filament on the Silicon structure.

The innovation described in this paper is intended as a low power broadband calibration light source for advanced optical sensors. Such a microsize lightsource would dramatically decrease power consumption of state-of-the-art calibration devices and therefore lead to easier integration to space vehicles. The limiting parameter for the current design is the attachment point of the filament to the package, which must be kept below 450 °C to avoid melting the solder material.

There were two separate analyses performed. The first was an analysis of the filament in a test fixture for the purpose of correlating a simple thermal model to test data. The second was a simple three-dimensional analysis of a package to show the impact of the hot filament on the Silicon package.

Functional details of this concept have been discussed in a past publication [1]. The thermal analysis of a preliminary design completely omitted the filament thermal requirements

and focused on the temperature prediction of a micro detector intended as a feedback loop to monitor the light [2]. At that time, the detector temperature requirements were the limiting factor in assessing the thermal integrity of the design. With the present design, it is felt that the filament will now be the limiting factor in the overall package thermal design.

MODELING TOOLS

Systems Improved Numerical Differencing Analyzer (SINDA) is a very popular tool used in common spacecraft thermal analyses. In spacecraft thermal design analysis, heat conduction and radiation are the dominant heat transfer mechanisms. SINDA is optimized for finite difference solutions to these types of problems on a spacecraft level. This paper is an interesting demonstration of the use of SINDA on a MEMS level. There are several versions of SINDA, and the one from SpaceDesign was chosen for convenience [3].

FILAMENT GEOMETRY AND MODEL

The tungsten filament, as shown in Figure 1, is shaped in a double spiral coil to provide a bright uniform light "point" source. The relationship between radius and spiral angle is

$$r = \frac{100\theta}{\pi} \quad (1)$$

The filament is 50 microns in width and 25 microns in thickness, with a 1.5 cm uncoiled length. For thermal analysis purposes, this can be assumed a straight line with total length 1.5 cm. The double spiral is symmetrical about the central point. The hottest point will be in the center of the 1.5 cm filament. A close examination of the filament geometry shows there is a length difference of about 18% between the outer wall filament path length and the inner wall filament path length. The outer path length calculates to be 1.649 cm and the inner path length 1.367 cm, yielding an average path length of 1.5 cm. It was the average path length that was used in this one-dimensional thermal analysis of the filament.

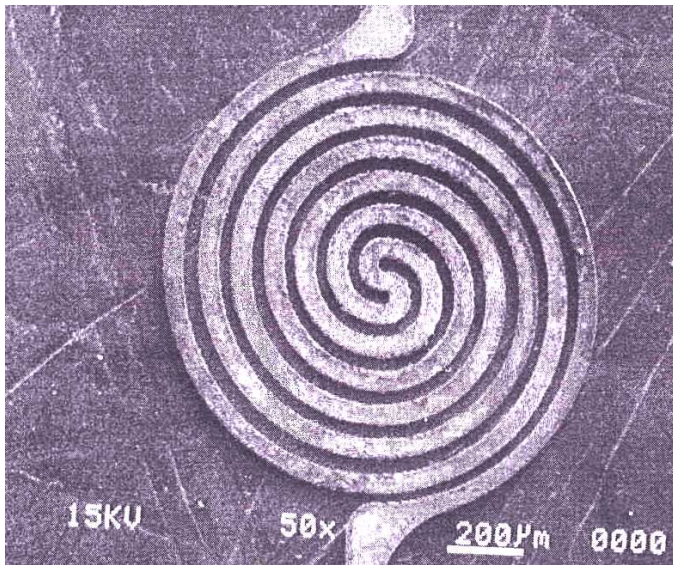


Figure 1. Scanning Electron Micrograph of the Filament

FILAMENT ANALYSIS

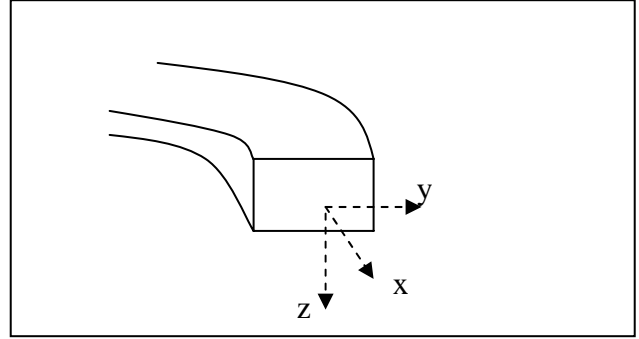


Figure 2. Coordinate System for Thermal Analysis

The temperature gradient of the thin filament in the z or y directions as shown in Figure 2 is negligible compared to the temperature gradient in the x direction. The maximum length in the y direction is 25 microns, and the maximum length in the z direction is 12.5 microns. The x direction is along the length of the filament with $x = 0$ at the center and $x = 0.75$ cm at the end of the spiral, as shown in Figure 3. As justification for this assumption, a calculation shows that the external radiation thermal conductance in the y or z directions, is small compared to the internal thermal conductance [4].

$$\frac{\sigma \varepsilon T^3 y}{k} \ll 1 \quad (2)$$

$$\frac{\sigma \varepsilon T^3 z}{k} \ll 1 \quad (3)$$

Thus, the only significant thermal gradients within the filament will be those along its length.

The analysis assumes steady state conditions. The governing equation for the filament is adapted from Carslaw and Jaeger [5] for a thin, high temperature wire carrying electricity as

$$\frac{d^2 T}{dx^2} - \frac{\varepsilon 2w\sigma(T^4 - T_o^4)}{kA_x} + \frac{\dot{q}}{k} = 0, \quad (4)$$

with boundary conditions $\frac{dT}{dx} = 0$ at $x = 0$,

and $T = 36^\circ\text{C}$ at $x = 0.75$ cm,

where

$$\dot{q} = f(T) \quad (5)$$

$$k = f(T) \quad (6)$$

$$\varepsilon = f(T) \quad (7)$$

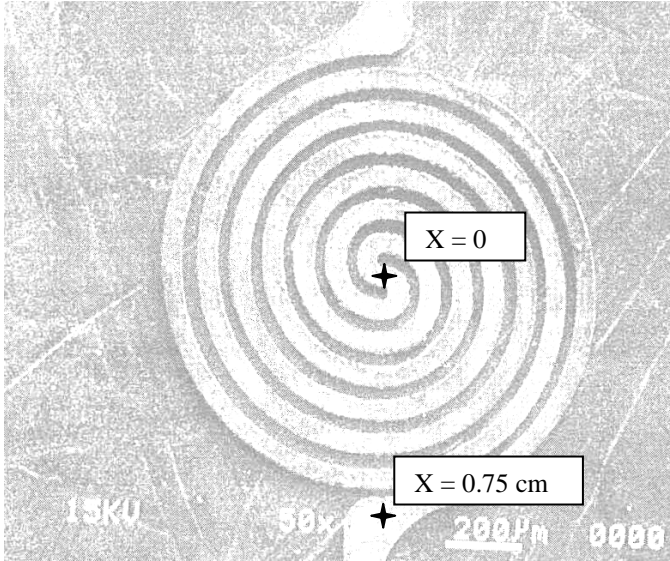


Figure 3. Thermal Analysis Coordinates on the Spiral

The filament symmetry required that only one half of the filament be modeled. Since the expected temperature range was from 2650 K to room temperature, temperature dependant properties of thermal conductivity, thermal emittance, and electrical resistivity were used.

The model divides the 0.75 cm length into 20 nodes. SINDA uses a standard finite difference scheme to solve the conduction and radiation problem. Since the test occurred in vacuum, no convection analysis was necessary. The vacuum chamber was at about room temperature, so the radiation heat sink, T_o , was held to 21 °C. Since the SINDA model only included one half of the filament, the temperature of one end of the filament represented the filament center and was allowed to come to equilibrium. The temperature of the other end was held to 36 °C. The fixture block was tactily estimated to be at a temperature on the order of 30 C suggesting that the block was in lesser thermal contact with the chamber than expected. The estimated 6 °C difference was considered to be much less than the 2650 K filament, so the model's 36 °C constraint was considered to be valid for correlation with the test data.

For future test data with possibly different filament geometries, the attach point temperature will be monitored with a small gauge thermocouple. The thermal contact resistance was assumed zero, since the contact pressure of these clamps was very high. The heat load was applied to each node as a function of the independent variable, current.

In the model, the independent variable, current, was adjusted until the thermal model current value matched the test value. Then, a heat balance was performed on the radiation and conduction heat transfer from the filament to determine the total heat loss predicted by the model. This was compared to the test electrical power measured during the test. Next, the model prediction of filament temperature was derived from a

fourth power average of all the individual nodal temperatures that were above the sensitivity of the Ircon Thermometer, 1500 °C. Then, this average filament temperature was compared to the test temperature recorded by the Ircon thermometer. Temperature dependent properties include conductance, electrical resistance, and emittance of Tungsten.

For thermal conductivity, Figure 4 shows that including temperature dependant properties are necessary, since the variation is large over the temperature range of interest.

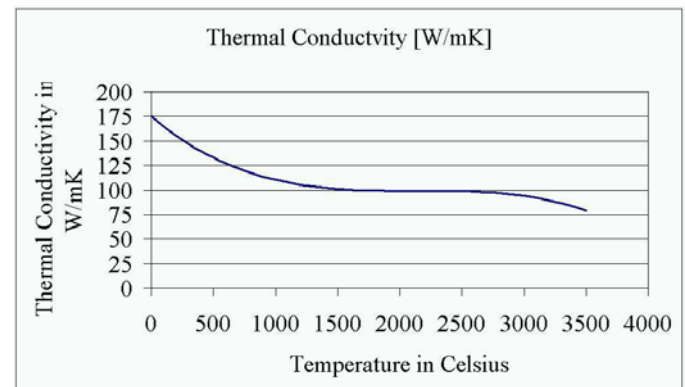


Figure 4. Plot Showing Tungsten Filament Thermal Conductivity Variation with Temperature

Heat generation is a function of temperature since Tungsten electrical resistivity varies with temperature substantially from 21 °C to 2650 K [6]. The temperature polynomial that describes this dependence is given below:

$$\rho = 4.6122 + 2.4498 \cdot 10^{-2} T + 3.5628 \cdot 10^{-6} T^2 - 1.9686 \cdot 10^{-10} T^3$$

Thermal radiative emittance of Tungsten is also a function of temperature [7]. It is approximately linear from 0.022 at 21 °C to 0.334 at 2727 °C.

Radiation thermal analysis assumed temperature dependent gray surfaces. The only radiating surfaces were the top and bottom of each filament section. Radiation between the filament segments to other filament segments was neglected, since the temperatures are nearly the same, and the principal path of radiation heat transfer is from the filament to the ambient surroundings at 21 °C. Thus, by using this approach, complicated radiation exchange factors representing heat transfer between the coil segments is not needed, and the model is very much simplified.

FILAMENT TESTING

The temperature of the filament was measured with an infrared thermometer, Ircon Modline 3R-35C15 [8], with the spectral region chosen to detect temperatures from 1500 °C to 3500 °C. The sensor uses a ratio radiation two-color technique to determine temperature.

Testing of the filament took place under vacuum with the filament structure firmly clamped between two electrodes that are shown in Figure 5.



Figure 5. Filament Test Mounting Fixture

PACKAGE GEOMETRY

The package geometry for a candidate design is shown in Figure 6. Although not to scale, relative positions of the window, filament and Silicon package are apparent.

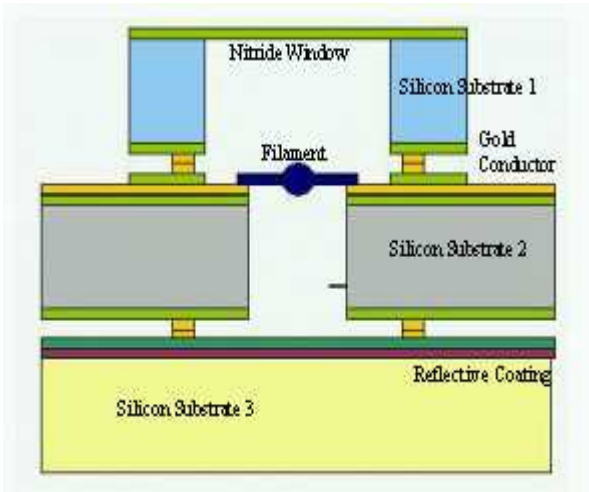


Figure 6. MEMS Package and Filament Geometry

The packaged device measures approximately 1.2 mm thick by 8 mm length and 5.4 mm width. The top of the device is covered by a thin (2.5 micron) Silicon Nitride (Si_3N_4) window, which is transparent to light. Several alternating layers of Si_3N_4 and Silicon (Si) form a sandwich structure that provides support for the filament, the Si_3N_4 window, and the electrical interconnects.

PACKAGE ANALYSIS

After a suitable model of the filament was obtained, the effect of the filament upon the package was determined. The package analysis was an application of SINDA in a three-dimensional conduction problem with temperature dependent conductivity. The package bulk temperature was expected to be near room temperature except for a local hot spot near the

filament attach point. The symmetry of the problem required that only one quarter of the package be modeled to adequately map the heat flow within the package. Thermal radiation was neglected, as this would give a maximum worst case hot spot on the package filament attach point. The amount of heat dissipated by the filament was applied to the attach point of the package. The bottom surface of the package was held to 21 °C. The two separate models were iterated until the attach point temperature and heat flow agreed in both models. In the package analysis, the filament attach point temperature was allowed to vary, and the resulting temperature was used as the input to the filament analysis.

This assumption of a fixed room temperature boundary condition of 21 °C is valid, since the attach point to a spacecraft would most likely be the spacecraft main bus or main payload structure. With the small heat load of this device, the spacecraft structure temperature would most likely be unaffected and act as an infinite “heat sink”. Room temperature is not an unreasonable assumption for spacecraft structure that is well insulated and in good thermal contact with the internal spacecraft environment. When actual spacecraft integration occurs, real “cold case” and “hot case” boundary conditions will be established.

RESULTS

Table 1 lists the model results versus the test data. It appears that the filament modeling is successful, as the test data matches the computer model results fairly well. Figure 7 shows the temperature versus filament length from the center of the filament to the edge attach point, as predicted by the model. A fourth power averaging scheme for each nodal temperature in the Ircan sensor range was used to get a representative average filament temperature. This was necessary because the infrared thermometer sensor measures the average temperature of the source, and is sensitive only to radiation between 1500 °C and 3500 °C [8].

Table 1. Filament Analysis Results

	Test	Model	Delta [%]
Power [Watts]	1.334	1.383	3.7
Temperature [°C]	2276	2340	2.5
Current [Amps]	0.4123	0.4123	N/A

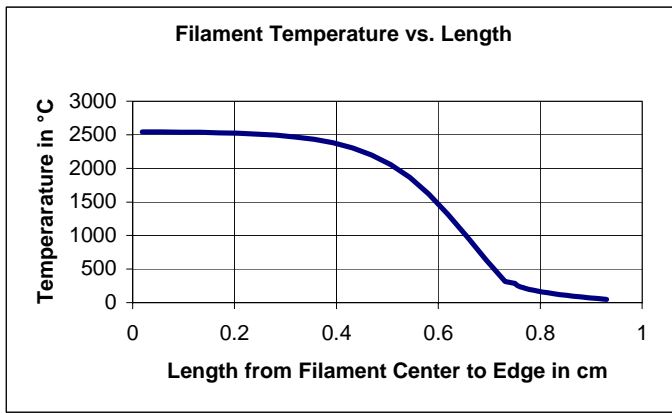


Figure 7. Temperature Plot as the Filament Spirals Outward
The package analysis showed that the filament attach point will be well below the 450 °C requirement. The attach point predicted temperature is 36 °C. This was subsequently used in the filament analysis as a boundary condition. The attach point is shown in Figure 8 as the hotspot near the corner.

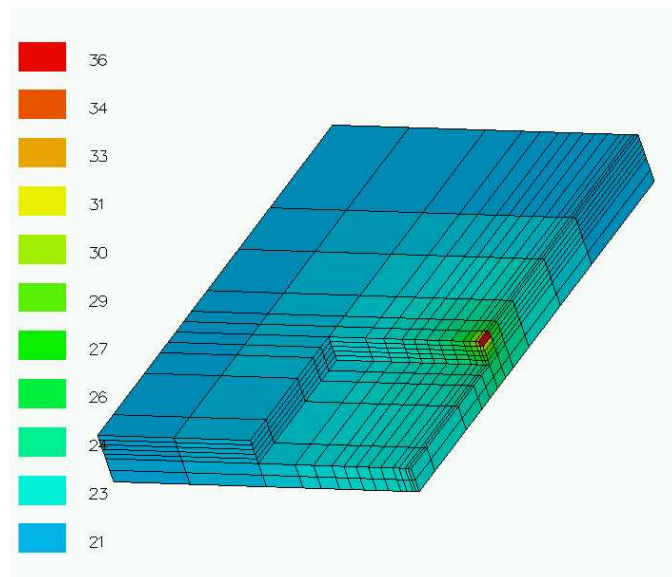


Figure 8. Package Analysis Results in °C

CONCLUSIONS

Common thermal analysis codes appear to be adequate to predict temperature results of MEMS devices on this scale. With the assumptions made here, the device will not exceed temperature requirements. Radiation modeling that only includes the top and bottom of the filament surface appears to be a valid approach. This greatly simplifies the thermal model thereby saving computational time and modeling effort. Also, the model provides a prediction of temperature versus filament length, something that is not available from testing due to instrumentation limitations.

SUMMARY

This paper has demonstrated the use of a standard thermal code to analyze and provide design recommendations for the development of a MEMS-based broadband light source. Although the small dimensions encountered in this problem are not typical of those solved by spacecraft thermal engineers, a thermal code typically used in spacecraft thermal analysis (SINDA), can be used. It appears that no microscale heat transfer effects are present. Since the data matched the thermal analysis predictions within an acceptable margin of error, it appears that a relatively simple thermal model is all that is needed to adequately predict current, power and temperature of the filament in the test fixture. Further thermal modeling and test data comparison is planned in the near future, as more test data becomes available. The model will be exercised for various filament designs and manufacturing techniques. As such, this report validates only a thermal model of a preliminary design, but indicates that the thermal modeling approach is sound.

ACKNOWLEDGEMENTS

The authors would like to acknowledge the research of Sue Wrbanek at NASA Glenn Research Center (GRC) and Drago Androjna of AKIMA, whose efforts made the Scanning Electron Micrographs of the Tungsten filament available for this report.

REFERENCES

- [1] M. Tuma, et al., "MEMS Incandescent Light Source," Proc. *SPIE Annual Meeting: Photonics for Space Environments VIII* (AM106) San Diego, CA., 2000.
- [2] E.L. Gollither, "Thermal Analysis of a MEMS Broadband Lightsource," Proc. *11th Thermal & Fluids Analysis Workshop*, Cleveland, Ohio, August, 2000.
- [3] J. Clay, "TSS User's Guide," www.spacedesign.com.
- [4] F. Incropera and D. DeWitt, *Fundamentals of Heat and Mass Transfer*, John Wiley & Sons, 1985
- [5] H.S. Carslaw and J.C. Jaegar, "Conduction of Heat in Solids Second Edition," pp.149-161, Oxford Science Publications, 1988.
- [6] J. Davis, *ITER Materials Handbook*, <http://aries.ucsd.edu/LIB/PROPS/ITER/AM01/AM01-0000.html>.
- [7] Y. S. Touloukian and D.P.DeWitt, "Thermophysical Properties of Matter," IF/Plenum Publishing, 1970.
- [8] Ircon, Inc., "Modline 3 Infrared Thermometer Installation/Operation Manual," IRCON, Inc., Niles, Illinois, March 2000.